DOI: 10.1002/zaac.200500483

Structure and Mössbauer Study of the First Mixed-Valence Iron Diphosphonate: $^{2}_{\infty}[\{Fe^{II/III}(H_2O)_2\}\{Fe^{III/II}Cl\}_2(\mu_4\text{-}O_3P\text{-}C(OH)\{(CH_2)_4NH_3\}\text{-}PO_3)_2]\cdot 4H_2O$

Khalid Abu-Shandi[a], Heiner Winkler[b], and Christoph Janiak[a,*]

[a] Freiburg, Universität, Institut für Anorganische und Analytische Chemie
[b] Lübeck, Universität, Institut für Physik

Received December 9th, 2005.

Abstract. The title compound bis(μ_4-5-ammonio-1-hydroxypentylidene-1,1-bisphosphonato-$\kappa^7O,O',O'',O''',O'^{v},O^{v},O^{v'},O^{v''}$)-(diaquairon)-di(chloroiron)(II/III)-tetrahydrate was prepared by hydrothermal synthesis and consists of nets of corner sharing $\{FeO_6\}$ or $\{FeClO_5\}$ octahedra linked by $\{CPO_3\}$ tetrahedra. Neighboring layers interdigitate with their ammoniopentylidene tails and connect to a three-dimensional network by N-H···O and O(hydrate)-H···O hydrogen bonds. The ligand $[PO_3\text{-}C(OH)\{(CH_2)_4{}^{+}NH_3\}\text{-}PO_3]^{3-}$ is a zwitter-ion of overall charge −3. Different from other known iron diphosphonates, which contain only either Fe^{II} or Fe^{III}, the iron bisphosphonate here is found from Mössbauer-Spectroscopy to be a trapped mixed-valence system with Fe^{II} and Fe^{III} disordered over both crystallographic sites Fe1 and Fe2 in what could be described as a coherent superposition of different states. At 4.2 K the Fe^{III} is completely magnetically ordered.

Keywords: Iron; Diphosphonate; ^{57}Fe Mössbauer spectroscopy; Organic-inorganic hybrid; Mixed-valence

Introduction

Metal organophosphonate compounds are multifunctional organic-inorganic hybrid materials and as open frameworks can be regarded in between zeolite-like and metal-organic framework materials [1]. The great interest in microporous materials, including metal (di)phosphonates comes from their potential applications in catalysis, ion exchange, proton conduction, absorption, gas storage and separation [2−5]. Organo(di)phosphonates (Scheme 1) can include various groups such as carboxylate, hydroxyl or amino in the organomoiety which presents a tunable functionality with a wide variety of structural motifs and properties [6]. Diphosphonates also play a role in biological systems, including the removal of iron from iron proteins [7]. The compound 3-ammonio-1-hydroxypropylidene-1,1-bisphosphonate (= pamidronate, Scheme 1) as the disodium salt is used clinically in the diagnosis and treatment of diseases affecting bone tissue [8, 9]. Following a report on Fe^{II}-pamidronate [10] we describe here the synthesis, structure and ^{57}Fe Mössbauer study of the iron compound with the related 5-ammonio-1-hydroxypentylidene-1,1-bisphosphonate, $\mathbf{1}^{3-}$.

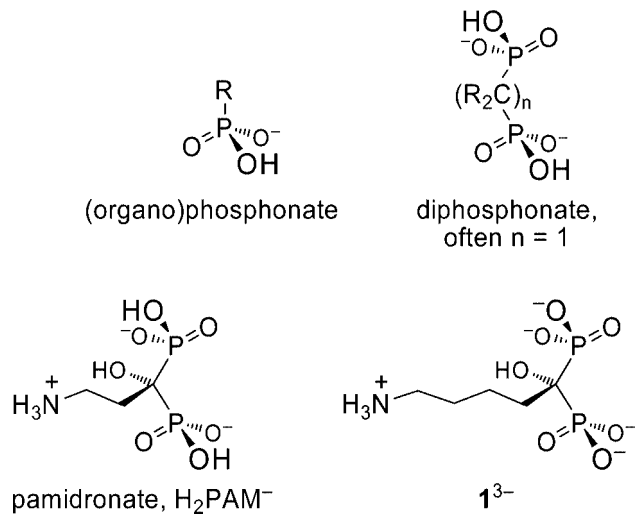

Scheme 1

Results and Discussion

The iron salt of $\mathbf{1}^{3-}$ (denoted as **2**) is obtained from the disodium trihydrate of (H-**1**)$^{2-}$ and iron(II) chloride in water under argon and hydrothermal conditions as dark green crystals. The proton in the hydrogen-bisphosphonate (H-**1**)$^{2-}$ oxidizes part of the Fe^{II} to Fe^{III} to give the ligand as $\mathbf{1}^{3-}$. Since the occupation factors of any protic hydrogen atoms and the Fe oxidation states are closely related [11], the single-crystal X-ray structure refinement alone usually cannot lead to an unambiguous formula assignment but needs the support by a ^{57}Fe Mössbauer study. The Mössbauer spectrum of **2** at room-temperature and 77 K (Fig. 1a and b) can be fitted by four doublets, two narrow ones which can be assigned to high-spin Fe^{III} (S = 5/2) and two wide ones assigned to high-spin Fe^{II} (S = 2) for both of which the observed isomer shifts and quadrupole splittings (Table 1) are typical. Subspectra with isomer shifts $\delta^{\alpha\text{-Fe}}$

* Prof. Dr. Chr. Janiak
Institut für Anorganische und Analytische Chemie
Universität Freiburg
Albertstr. 21
D-79104 Freiburg
E-Mail: janiak@uni-freiburg.de

below 0.7 mm s^{-1} are assigned to Fe^{III}, those above 1 mm s^{-1} to Fe^{II} [4, 11, 12]. The decrease in the isomer shifts from 77 K to RT follows from the second-order Doppler shift (SOD). The slight decrease in ΔE_Q from 77 K to RT is explained by a shift in the thermal Boltzmann distribution leading to the beginning occupation of excited states by which the electron distribution becomes more spherical. At 4.2 K (Fig. 1c) most of the iron ions are magnetically ordered as is evident by the appearance of the magnetic sextets and the absence of the narrow doublets. The large magnetic splitting around 50 Tesla is again consistent with Fe^{III}. The disappearance of the quadrupole splittings for the magnetic sextetts (Table 1) may be explained with the magic angle θ between the electric field gradient and the magnetic hyperfine field according to $3\cos^2\theta - 1 = 0$. The remaining area at 4.2 K can be fitted by a broad wide doublet (Fig. 1c, Table 1) with $\delta^{\alpha\text{-Fe}}$ and ΔE_Q similar to one of the two Fe^{II} doublets observed at higher temperature. The fractional area of the nonmagnetic doublet at 4.2 K is only a lower limit because it is hard to determine how much of it is buried under the magnetic sextets. For similar reasons only one very broad doublet has been allowed for since a reliable separation into two doublets seems unfeasible. Part of the intensities of the wide doublets may have also been shifted to the magnetic sextets, that is both the Fe^{III} and Fe^{II} become magnetically ordered. At room temperature and 77 K we have two Fe^{III} and two Fe^{II} doublets. The Fe^{III} doublet with the larger quadrupole splitting ΔE_Q (subspectrum 2) is assigned to the more distorted iron site Fe2 as $Fe2^{III}$, the Fe^{III} doublet with the smaller ΔE_Q (subspectrum 1) is assigned to the higher symmetrical Fe1 (located on center of inversion, Wyckoff site symmetry 1g) as $Fe1^{III}$. Similarly, the Fe^{II} doublet with the larger ΔE_Q (subspectrum 3) is assigned to Fe2 ($Fe2^{II}$), the one with the smaller ΔE_Q (subspectrum 4) to Fe1 ($Fe1^{II}$). The finding of a Fe^{II} and Fe^{III} site for both Fe1 and Fe2 leads to the interpretation of **2** as a trapped mixed-valence system on the time scale of a Mössbauer experiment of 10^{-7} s [13]. We see no intervalence transition between Fe^{II} and Fe^{III}, that is, no detrapping of the localized valence states [11, 14]. The ratio of the relative areas $A_{Fe(III)}/A_{Fe(II)}$ is about 2.8:1 which is higher than the ratio of 2:1 for the different iron sites seen in the crystal structure (see below). In part this may be explained by an expected somewhat higher recoil-free fraction for the Fe^{III} sites. Alternatively, the discrepancy may be rationalized by the presence of isostructural phases with different proton contents in the sample used for the Mössbauer study. A phase with a smaller proton content, that is, deprotonation of $-NH_3^+$ to $-NH_2$ or aqua ligand $-OH_2$ to hydroxo group $-OH^-$ is associated with a larger amount of Fe^{III} [15].

The structural investigation of **2** shows two crystallographically different iron sites in a 2:1 ratio (Fe2:Fe1): The site for Fe1 coincides with the inversion center at 0, 1/2, 1/2. Both sites are octahedrally coordinated with four oxygen atoms from bisphosphonate ligands. For Fe1 these four O atoms come from two chelating bisphosphonate ligands,

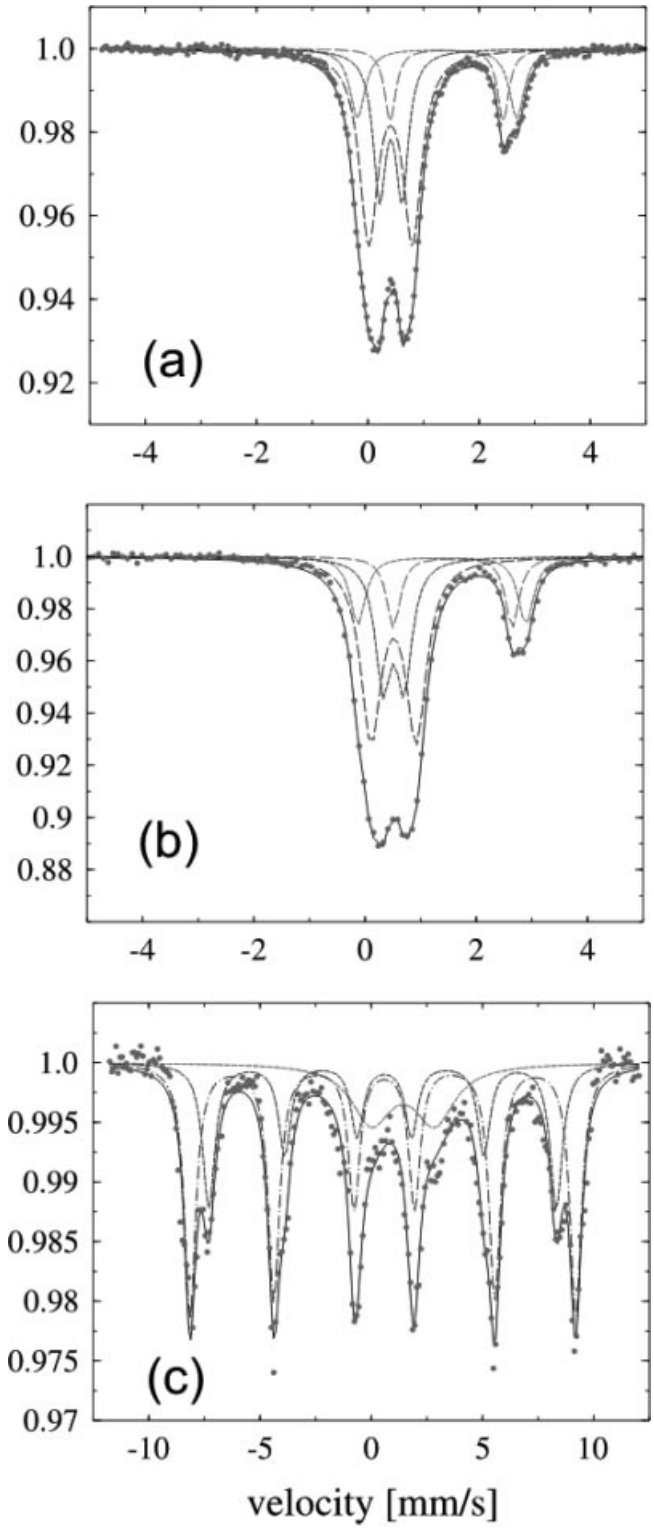

Fig. 1 Mössbauer spectrum of **2** at (a) room temperature, (b) T = 77 K and (c) 4.2 K. A sum of Lorentzians (solid line, parameters in Table 1) is used to fit the experimental data (dots) (note the different scale on the abscissa for c).

and two *trans* aqua ligands complete the coordination sphere (Fig. 2). For Fe2 these four O atoms stem from one

Table 1 Mössbauer parameters for compound **2** [a]

Temp. /K	Subspectrum	$\delta^{\alpha\text{-Fe}}$ [b] /mm s^{-1}	ΔE_Q [c] /mm s^{-1}	B_{hf} [d] /Tesla	rel. area A/%	Interpretation Fe-oxid.	site
293	1 narrow doublet	0.41 [e]	0.40	–	25.4	III	Fe1
(RT)	2 narrow doublet	0.41 [e]	0.79	–	48.5	III	Fe2
	3 wide doublet [f]	1.25	2.86	–	14.7	II	Fe2
	4 wide doublet [f]	1.42	2.03	–	11.4	II	Fe1
77	1 narrow doublet	0.51 [e]	0.38	–	25.1	III	Fe1
	2 narrow doublet	0.51 [e]	0.81	–	48.4	III	Fe2
	3 wide doublet [f]	1.38	3.02	–	13.8	II	Fe2
	4 wide doublet [f]	1.58	2.14	–	12.7	II	Fe1
4.2	1 magnet. sextet	0.55	−0.08	47.9	28.6	III	Fe1
	2 magnet. sextet	0.56	−0.06	53.2	54.3	III	Fe2
	3 wide doublet	1.43	2.85	–	17.1	II	Fe1,2

[a] The errors of the hyperfine parameters are about 2 % and of the relative areas 5 %. [b] Isomer shift. [c] Quadrupole splitting. [d] Magnetic hyperfine field. [e] Parameters kept equal during the fitting to limit the number of free parameters. [f] The two wide doublets were fitted to a similar isomer shift and different quadrupole splitting.

chelating bisphosphonate and two different bridging phosphonate groups. The coordination of Fe2 is completed by a chloro ligand and coordination of the alcoholic oxygen atom from **1**.

Bond valence sum calculations [16, 17] for the iron atoms in **2** based on the Fe−O and Fe−Cl distances of the single-crystal structure analysis give a value of 2.064 or 2.208 for Fe1 (as Fe^{II} or Fe^{III}, respectively) and of 3.004 or 2.849 for Fe2 (as Fe^{III} or Fe^{II}). This suggests Fe1 to be primarily in the +II and Fe2 in the +III oxidation state. None of the phosphonate oxygen atoms was found to be protonated. Protonated O atoms would also be recognized by their longer P−O distance of 1.562-1.578 Å, versus 1.494-1.516 Å for unprotonated O atoms [9, 18]. In **2** the P−O distances range from 1.499(2) to 1.544(2). Therefore, each zwitter-ionic ammonio-bisphosphonate anion was assigned as triply negative as depicted in Scheme 1. The total charge of 8− from 2×**1**$^{3-}$ and 2 Cl^- ligands is balanced by the positive charge from 1×Fe^{2+} and 2×Fe^{3+}. The results of the bond valence sum calculations based on the bond distances in the single-crystal structure, which indicate that Fe1 is divalent and Fe2 is trivalent, are at variance with the above Mössbauer measurements, which interpret both Fe1 and Fe2 to be in a trapped mixed-valence state. Finding only one position for Fe1 and Fe2, respectively, suggests a coherent superposition of the different states $Fe1^{II}(Fe2a^{III}Fe2b^{III})$, $Fe1^{III}(Fe2a^{II}Fe2b^{III})$ and $Fe1^{III}(Fe2a^{III}Fe2b^{II})$ in a superstructure for **2**. X-ray crystallography averages the electron density distributions to yield crystallographically identical iron positions for $Fe1^{II}$ and $Fe1^{III}$ (as well as for $Fe2^{II}$ and $Fe2^{III}$) while the Mössbauer hyperfine parameters reveal primarily the electronic and not the real structure. A very similar situation was described for the compound $(C_4H_{12}N_2)[Fe_4(OH)_2(HPO_4)_5]$ with also two crystallographically different iron sites Fe1 and Fe2 (in a 1:1 ratio) having both approximately the same charge distribution of 30 % Fe^{II} and 70 % Fe^{III} (note also the excess of Fe^{III}) while bond valence sum calculations (clearly) indicated Fe1 as trivalent and Fe2 as divalent [15].

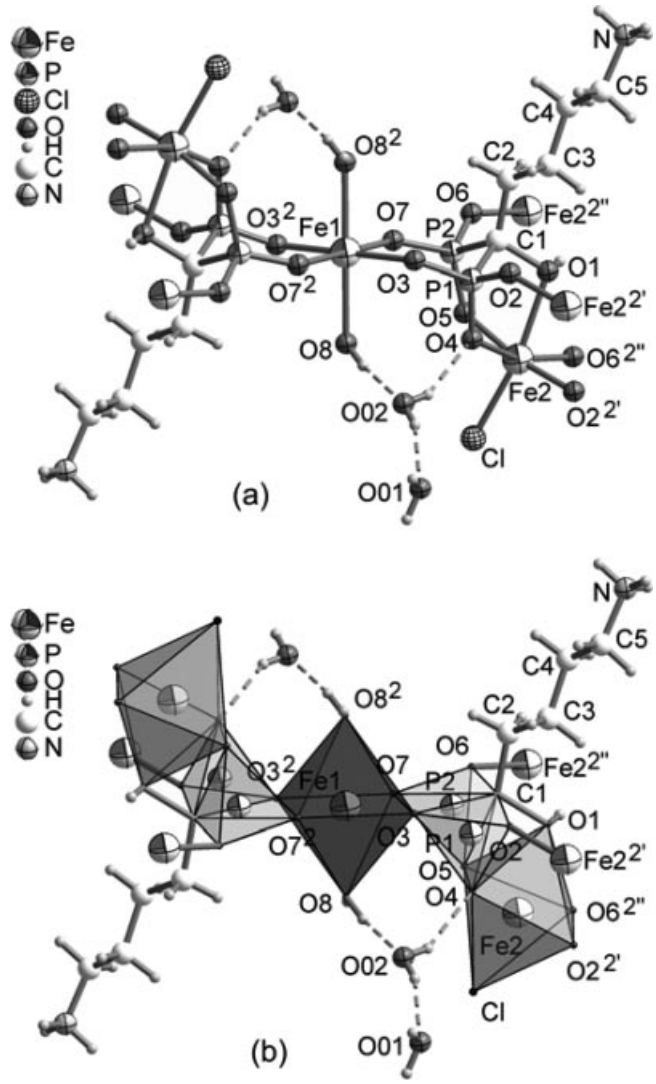

Fig. 2 Formula unit of **2**, with the two different iron atoms Fe1 and Fe2 (1:2 ratio) and two chelating and bridging bisphosphonate ligands. The bridging action is emphasized by showing the symmetry related iron atoms $Fe2^{2'}$ and $Fe2^{2''}$. Also shown is the water of crystallization with part of the hydrogen bonding interactions (details of the O−H···O, N−H···O and O−H···Cl bonds are included in the deposited cif-file). (a) Ball and stick representation, (b) Polyhedral representation around the Fe and P atoms (with O atoms contracted).
Selected distances/AÅ and angles/°: Fe1−O3 2.076(2), Fe1−O7 2.090(2), Fe1−O8 2.243(2); Fe2−O1 2.290(2), Fe2−$O2^{2'}$ 1.931(2), Fe2−$O6^{2''}$ 1.975(2), Fe2−O4 1.991(2), Fe2−O5 2.072(2), Fe2−Cl 2.2884(9); *cis* O−Fe1−O 87.82(7)-92.18(7), *cis* O−Fe2−Cl 91.22(5)-99.13(6), O1−Fe2−$O2^{2'}$ 93.27(7), O1−Fe2−$O6^{2''}$ 83.29(7), O1−Fe2−O4 79.28(7), O1−Fe2−O5 77.73(6), other *cis* O−Fe2−O 87.25(7)-92.03(7), O4−Fe2−$O6^{2''}$ 162.51(7), $O2^{2'}$−Fe2−O5 170.95(7), Cl−Fe2−O1 168.74(5); symmetry relations 2 = $-x$, $1-y$, $1-z$; 2′ = $-x$, $1-y$, $2-z$; 2″ = $1-x$, $1-y$, $2-z$.

The crystal structure of **2** is built from layers of alternating corner sharing $\{FeO_6\}$ or $\{FeClO_5\}$ octahedra and $\{PO_3C\}$ tetrahedra (Fig. 3 and 4). The layers lie parallel to the *ac*-plane. Along *b*, neighboring layers interdigitate with their ammonio-pentylidene residues through N-H···O hydrogen bonding interactions to give a three-dimensional

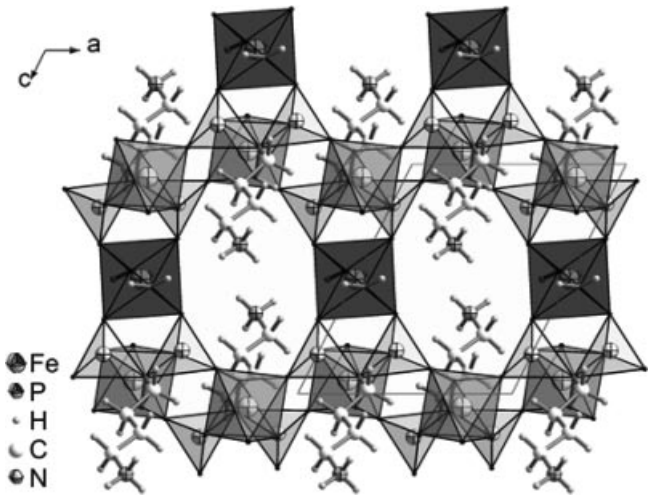

Fig. 3 Section of an individual layer in **2**. Polyhedral representation (with O atoms contracted) around the Fe and P atoms. Fe1 polyhedra in dark gray, Fe2 polyhedra in light gray.

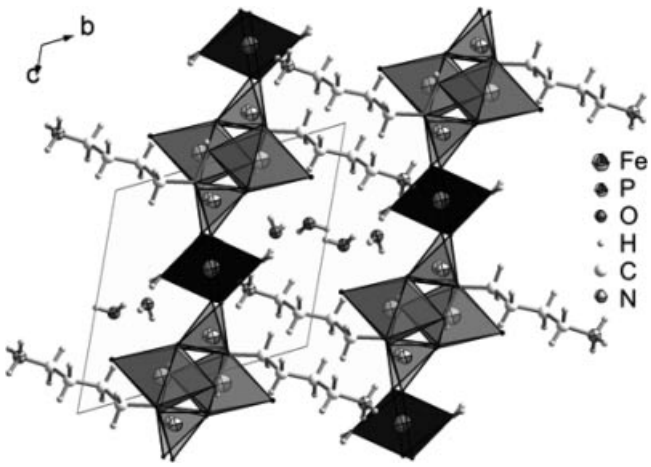

Fig. 4 Interdigitation of neighboring layers along *b* with the layers projected on the *bc* plane. Hydrogen bonds are not shown for clarity. Details of the O−H···O, N−H···O and O−H···Cl bonds are included in the deposited cif-file.

supramolecular network. Voids in between the layers and the residues are filled with water molecules of crystallization (Fig. 4).

There is only a limited number of iron diphosphonates described, so far, possibly due to the oxidation state ambiguity [19]. The structure of mixed-valence **2**, $^{2}_{\infty}$[{$Fe^{II/III}(H_2O)_2$}{$Fe^{III/II}Cl$}$_2$(μ_4-O_3P-C(OH){$(CH_2)_4NH_3$}-PO_3)$_2$]·4H_2O can be compared to $^{2}_{\infty}$[$Fe^{III}_2(H_2O)_2$(O_3P-CH_2-PO_3H)$_2$]·2H_2O (MIL-13) [19c], $^{1}_{\infty}${[$H_3N(CH_2)_n$-NH_3][Fe^{II}_2(O_3P-C(OH)(CH_3)-PO_3H)$_2$]·2H_2O} (n = 2, 4) [19b, d], $^{1}_{\infty}${[$H_3N(CH_2)_2NH_2(CH_2)_2NH_3$][$Fe^{III}$($O_3$P-C-(OH)($CH_3$)-$PO_3H$)$_2$]·2$H_2O$} [19b] and $^{3}_{\infty}$[$Fe^{III}(H_2O)$(O_3P-CH_2-PO_3H)] [19a]. Different from **2**, the iron ions in all of these structures are either in the +2 or +3 oxidation state. Hence, **2** appears to present the first mixed-valence iron-(II/III) diphosphonate.

Experimental Section

General procedures

All work involving air- and/or moisture-sensitive compounds was carried out by using standard vacuum and Schlenk techniques. IR spectra (KBr pellet) were measured on a Bruker Optik IFS 25. NMR spectra were recorded with a Bruker Avance DPX200 spectrometer at 300 K (200 MHz for ^{1}H, 81 MHz for ^{31}P with ^{1}H broad band decoupling) with calibration against the solvent signal (D_2O 4.87 ppm) or an external standard of 85 % H_3PO_4, respectively. Elemental analyses were obtained on a VarioEL from Elementaranalysensysteme GmbH. ^{57}Fe Mössbauer spectra were recorded with a conventional spectrometer in constant-acceleration mode with a ^{57}Co[Rh] source. The velocity calibration was performed with an α-Fe foil at room temperature, for which the magnetic hyperfine splitting is known with high accuracy. The measured isomer shifts are referred to this α-Fe standard. The experimental spectra were fitted by a sum of Lorentzian lines by means of a least-squares procedure. X-ray powder diffractometry was done on a Stoe STADI P with Debye-Scherrer geometry, Mo-Kα radiation (λ = 0.7093 Å) and a Ge(111) monochromator and the samples in glass capillaries on a rotating probe head.

The compound disodium (5-ammonio-1-hydroxypentylidene-1,1-bisphosphonate) trihydrate (= 5-amino-1-hydroxypentylidene-1,1-bisphosphonic acid disodium salt trihydrate), Na_2[H_3N-$(CH_2)_4$C(OH)(PO_3)(PO_3H)]·3H_2O, was prepared by the method of *Kieczykowski* and coworkers from 5-aminopentanoic acid, $H_2N(CH_2)_4COOH$ (5.58 g, 47.5 mmol), phosphonic acid, H_3PO_3 (4.0 g, 47.5 mmol) and trichlorophosphine, PCl_3 (8.75 ml, 100 mmol) [20]. The product was collected by filtration, washed with cold water and 95 % ethanol and dried at room temperature for one night (yield 9.0 g, 52 %). IR (major peaks only): ν = 3438 (br, νOH), 3253 (νNH), 3003 (νCH), 1670 (νC−C), 1476 (νP=O), 1041 cm^{-1} (νP−O). − ^{1}H NMR (D_2O): δ = 3.04 (t, CH_2, J = 5.6 Hz), 3.05 (br, NH_3), 1.95 (m, CH_2, J = 5.6 Hz), 1.2−1.7 (m, CH_2). − ^{31}P NMR (D_2O): δ = 18.63. − $C_5H_{19}NNa_2O_{10}P_2$ (361.13): calcd. C 16.63, H 5.30, N 3.88; found C 16.50, H 5.28, N 3.59 %.

Bis(μ-5-ammonio-1-hydroxypentylidene-1,1-bisphosphonato)-(diaquairon)-di(chloroiron)(II/III)-tetrahydrate (**2**): $FeCl_2$·4H_2O (0.35 g, 1.76 mmol) was dissolved in a Schlenk flask under a positive pressure of argon in 5 ml of degassed water to give a yellowish-green clear solution. To this solution the disodium bisphosphonate salt (0.645 g, 1.79 mmol) was added with continuous stirring. The pH value of the resulting solution was 3.65. The mixture was stirred at room temperature for 30 min. The solution was transferred to a Teflon-lined stainless steel autoclave and heated to 180 °C for 40 h followed by slow cooling at a rate of 10 °C/h. Dark green crystals were collected by filtration (yield 0.31 g, 40 %). IR (major peaks only): ν = 3414 (br, νOH), 3225 (νNH), 3115 (νCH), 1662 (νC−C), 1481 (νP=O), 995 cm^{-1} (νP−O). − $C_{10}H_{36}Cl_2Fe_3N_2O_{20}P_4$ (866.74): calcd. C 13.86, H 4.19, N 3.23; found C 13.96, H 4.44, N 3.20 %.

X-ray powder diffractometry shows the crystals of **2** to be a single phase.

Crystal structure determination of **2**: *Crystal data*: Molecular formula $C_{10}H_{36}Cl_2Fe_3N_2O_{20}P_4$, formula weight 866.74 g mol^{-1}, a = 8.1437(19), b = 10.318(2), c = 10.491(2) Å, α = 112.096(4)°, β = 112.377(3)°, γ = 94.629(4)°, V = 729.0(3) Å^3, Z = 1, D_{calc} =

1.974 g cm^{-3}, triclinic, space group $P-1$. *Data collection*: Bruker Smart AXS CCD, Mo−K_α radiation (λ = 0.71073 Å), graphite monochromator, crystal size 0.17x0.09x0.09 mm^3, 298(2) K, ω-scan, 4.4° ≤ 2θ ≤ 54.5°, −10 ≤ h ≤ 10, −13 ≤ k ≤ 13, −13 ≤ l ≤ 13, 6383 reflections measured, 3217 independent (R_{int} = 0.0179), μ(Mo−K_α) 1.961 mm^{-1}, F(000) 442; data collection and cell refinement with SMART [21], data reduction with SAINT [21], experimental absorption correction with SADABS [22]. *Structural Analysis and Refinement*: The structure was solved by direct methods (SHELXS-97), refinement was done by full-matrix least squares on F^2 using the SHELXL-97 program suite [23]. All non-hydrogen positions were found and refined with anisotropic displacement parameters. The hydrogen atoms on the aqua ligand (O8) and the water molecules of crystallization (O01, O02) were found from the difference Fourier map and their positions were refined isotropically with Ueq(H) = 1.5 Ueq(O). Hydrogen atoms on carbon, the oxygen atom of -COH and the ammonio-nitrogen atom were placed at calculated positions, using appropriate riding models (AFIX 23 for CH_2, AFIX 133 for NH_3 and AFIX 83 for -COH) and Ueq(H) = 1.2 Ueq(C) for CH_2 and Ueq(H) = 1.5 Ueq(N,O) for -COH and NH_3. 207 refined parameters, final *R1* = 0.0289, *wR2* = 0.0697 for 3217 reflections with $I > 2\sigma(I)$, final *R1* = 0.0396, *wR2* = 0.0744 for all data, goodness-of-fit 1.000, largest difference peak and hole 0.602/−0.454 e $Å^{-3}$. Graphics were obtained with DIAMOND (Version 3.0e) [24]. The structural data has been deposited with the Cambridge Crystallographic Data Center (No. CCDC-295018).

Acknowledgments. The research was supported by GABA Intl., Switzerland. We appreciate a fellowship to K.A-S. by the Graduate College "Unpaired electrons".

References

[1] Reviews: K. Maeda, *Microporous and Mesoporous Materials* **2004**, *73*, 47. A. Clearfield, Z. Wang, *J. Chem. Soc., Dalton Trans.* **2002**, 2937. A. Clearfield, *Curr. Opinion Sol. State Mat. Res.* **2002**, *6*, 495.

[2] Review: C. Janiak, *Dalton Trans.* **2003**, 2781.

[3] G. Alberti, U. Constantino, M. Casciola, R. Vivani, *Adv. Mater.* **1996**, *8*, 291. J. L. Snover, H. Byrd, E. P. Suponeva, E. Vicenzi, M. E. Thompson, *Chem. Mater.* **1996**, *8*, 1490.

[4] K. Abu-Shandi, H. Winkler, B. Wu, C. Janiak, *CrystEngComm* **2003**, *5*, 180.

[5] (a) R. Clarke, K. Latham, C. Rix, M. Hobday, J. White, *CrystEngComm* **2005**, *7*, 28; (b) S. Midollini, A. Orlandini, A. Vacca, *Inorg. Chem. Commun.* **2004**, *7*, 1113; (c) B.-P. Yang, Z.-M. Sun, J.-G. Mao, *Inorg. Chim. Acta* **2004**, *357*, 1583; (d) M. Riou-Cavellec, M. Sanselme, G. Férey, *J. Mater. Chem.* **2000**, *10*, 745.

[6] Recent references: (a) W. R. Gemmill, M. D. Smith, B. A. Reisner, *J. Solid State Chem.* **2005**, *178*, 2658; (b) G. Yucesan, V. Golub, C. J. O'Connor, J. Zubieta, *Dalton Trans.* **2005**, 2241; (c) Z. M. Sun, J. G. Mao, Z. C. Dong, *Polyhedron* **2005**, *24*, 571.

[7] (a) W. R. Harris, C. E. Brook, C. D. Spilling, S. Elleppan, W. Peng, M. Xin, J. Van Wyk, *J. Inorg. Biochem.* **2004**, *98*, 1824; (b) E. Gumienna-Kontecka, J. Galezowska, M. Drag, R. Latajka, P. Kafarski, H. Kozlowski, *Inorg. Chim. Acta* **2004**, *357*, 1632.

[8] Recent references: (a) G. Duque, R. Segal, J. Bianco, *J. Am. Geriatrics Soc.* **2005**, *53*, 1633; (b) T. J. Cho, I. H. Choi, Y. C. Chung, *J. Pediatric Orthopaedics* **2005**, *25*, 607; (c) S. C. L. M. Cremers, S. E. Papapoulos, H. Gelderblom, *J. Bone Mineral Res.* **2005**, *20*, 1543; (d) A. N. Toukap, G. Depresseux, J. P. Devogelaer, *LUPUS* **2005**, *14*, 517; (e) J. M. Stephens, M. S. Aapro, M. F. Botteman, *J. Clin. Oncol.* **2005**, *23*, 44S Part 1, Suppl.; (f) S. J. Jung, G. Hwang, Y. Lee, *J. Clin. Oncol.* **2005**, *23*, 99S Part 1 Suppl. S.

[9] (a) K. Stahl, S. P. Treppendahl, H. Preikschat, E. Fischer, *Acta Crystallogr.* **2005**, *E61*, m132; (b) D. Vega, D. Fernández, J. A. Ellena, *Acta Crystallogr.* **2002**, *C58*, m77; (c) D. Fernández, D. Vega, A. Goeta, *Acta Crystallogr. C* **2002**, *58*, m494.

[10] K. Abu-Shandi, C. Janiak, *Z. Naturforsch.* **2005**, *60b*, 1250.

[11] K. Abu-Shandi, H. Winkler, M. Gerdan, F. Emmerling, B. Wu, C. Janiak, *Dalton Trans.* **2003**, 2815.

[12] (a) K. Abu-Shandi, H. Winkler, H. Paulsen, R. Glaum, B. Wu, C. Janiak, *Z. Anorg. Allg. Chem.* **2005**, *631*, 2705; (b) B. Kersting, M. J. Kolm, C. Janiak, *Z. Anorg. Allg. Chem.* **1998**, *624*, 775.

[13] (a) B. Kersting, D. Siebert, D. Volkmer, M. J. Kolm, C. Janiak, *Inorg. Chem.* **1999**, *38*, 3871; (b) A. Geiss, M. J. Kolm, C. Janiak, H. Vahrenkamp, *Inorg. Chem.* **2000**, *39*, 4037.

[14] T. Manago, S. Hayami, H. Oshio, S. Osaki, H. Hasuyama, R. H. Herber, Y. Maeda, *J. Chem. Soc., Dalton Trans.* **1999**, 1001.

[15] V. Zima, K.-H. Lii, N. Nguyen, A. Ducouret, *Chem. Mater.* **1998**, *10*, 1914.

[16] Bond valences (s) calculated from the bond lengths (R) according to $s = \exp(R_0-R)/B$ and R_0 = 1.734 for Fe^{2+}−O, 1.759 for Fe^{3+}−O, 2.115 for Fe−Cl, B = 0.37. Program VALENCE (Version 2.00, February 1993). I. D. Brown, *J. Appl. Crystallogr.* **1996**, *29*, 479.

[17] (a) I. D. Brown, R. D. Shannon, *Acta Crystallogr.* **1973**, *A29*, 266; (b) I. D. Brown, K. K. Wu, *Acta Crystallogr.* **1976**, *B32*, 1957; (c) I. D. Brown, D. Altermatt, *Acta Crystallogr.* **1985**, *B41*, 244.

[18] E. Craven, K. Abu-Shandi, C. Janiak, *Z. Anorg. Allg. Chem.* **2003**, *629*, 195.

[19] (a) C. A. Merrill, A. K. Cheetham, *Inorg. Chem.* **2005**, *44*, 5273; (b) H.-H. Song, L.-M. Zheng, G.-S. Zhu, Z. Shi, S.-H. Feng, S. Gao, Z. Hu, X.-Q. Xin, *J. Solid State Chem.* **2002**, *164*, 367; (c) M. Riou-Cavellec, C. Serre, J. Robino, M. Noguès, J.-M. Grenèche, G. Férey, *J. Solid State Chem.* **1999**, *147*, 122; (d) L.-M. Zheng, H.-H. Song, C.-H. Lin, S.-L. Wang, Z. Hu, Z. Yu, X.-Q. Xin, *Inorg. Chem.* **1999**, *38*, 4618; (e) A. W. Herlinger, J. R. Ferraro, J. A. Garcia, R. Chiarizia, *Polyhedron* **1998**, *17*, 1471.

[20] G. R. Kieczykowski, R. B. Jobson, D. G. Melillo, D. F. Reinhold, V. J. Grenda, I. Shinkai, *J. Org. Chem.* **1995**, *60*, 8310.

[21] SMART, Data Collection Program for the CCD Area-Detector System; SAINT, Data Reduction and Frame Integration Program for the CCD Area-Detector System. Bruker Analytical X-ray Systems, Madison, Wisconsin, USA (1997).

[22] G. Sheldrick, Program SADABS: Area-detector absorption correction, University of Göttingen, Germany (1996).

[23] G. M. Sheldrick, SHELXS-97, SHELXL-97, Programs for Crystal Structure Analysis, University of Göttingen, Germany, 1997.

[24] DIAMOND 3.0e for Windows. Crystal Impact Gbr, Bonn, Germany; http://www.crystalimpact.com/diamond.

